Urrejola, C., von Dassow, P., van den Engh, G., Salas, L., Mullineaux, C. W., Vicuña, R., & Sanchez-Baracaldo, P. (2020). Loss of filamentous multicellularity in Cyanobacteria - the extremophile Gloeocapsopsis sp. UTEX B3054 retained multicellular features at the genomic and behavioral level. *Journal of Bacteriology*. https://doi.org/10.1128/JB.00514-19

Loss of filamentous multicellularity in Cyanobacteria - the extremophile *Gloeocapsopsis* sp. UTEX B3054 retained multicellular features at the genomic and behavioral level

Catalina Urrejola #[1], Peter von Dassow [1,2,3], Ger van den Engh [4], Loreto Salas[1], Conrad W. Mullineaux[5], Rafael Vicuña[1], Patricia Sanchez-Baracaldo #[6]

[1] Faculty of Biological Sciences, Pontificia Universidad Católica de Chile.
[2] Instituto Milenio de Oceanografía, Chile.
[3] UMI3614 Evolutionary Biology and Ecology of Algae, CNRS-UPMC Sorbonne Universités, PUCCh, UACH, Station Biologique de Roscoff, Roscoff, France.
[4] Center for Marine Cytometry, Concrete, WA, USA.
[5] School of Biological and Chemical Sciences, Queen Mary University of London, United Kingdom.
[6] School of Geographical Sciences, University of Bristol, BS8 1SS, United Kingdom.

Address correspondence to:
Currejol@uc.cl
P.Sanchez-Baracaldo@bristol.ac.uk

Running Head: Loss of filamentous multicellularity in cyanobacteria

Main text length: 4210 words

Abstract

Multicellularity in Cyanobacteria played a key role in their habitat expansion contributing to the Great Oxidation Event around 2.45–2.32 billion years ago. Evolutionary studies have indicated that some unicellular cyanobacteria emerged from multicellular ancestors, yet little is known about how the emergence of new unicellular morphotypes from multicellular ancestors occurred. Our results give new insights into the evolutionary reversion from which the *Gloeocapsopsis* lineage emerged. Flow cytometry and microscopy results revealed morphological plasticity, involving patterned formation of multicellular morphotypes sensitive to environmental stimuli. Genomic analyses unveiled the presence of multicellular-associated genes in its genome. Calcein-FRAP experiments confirmed that *Gloeocapsopsis* sp. UTEXB3054 carry out cell-to-cell communication in multicellular morphotypes, but in slower timescales than filamentous cyanobacteria. Although traditionally classified as unicellular, our results suggest that *Gloeocapsopsis* displays facultative multicellularity, a condition that may have conferred ecological advantages for thriving as an extremophile for more than 1.6 billion years.

Importance

Cyanobacteria are amongst the few prokaryotes that evolved multicellularity. The early emergence of multicellularity in Cyanobacteria (2.5 billion years ago) entails that some unicellular cyanobacteria reverted from multicellular ancestors. We tested this evolutionary hypothesis by studying the unicellular strain *Gloeocapsopsis* sp. UTEXB3054, using flow cytometry, genomics and cell-to-cell communication experiments. We demonstrated the existence of a well-defined patterned organization of cells in clusters during growth, which might change triggered by environmental stimuli. Moreover, we found genomic signatures of multicellularity in *Gloeocapsopsis* genome, giving new insights into the evolutionary history of a Cyanobacterial lineage that has thrived in extreme environments since the early Earth. The potential benefits in terms of resource acquisition and ecological relevance of this transient behavior are discussed.

Introduction

Cyanobacteria have fundamentally transformed the geochemistry and biodiversity on the Earth's surface. They are thought to be responsible for the rise of atmospheric oxygen levels during the Great Oxidation Event around 2.4-3.2 billion years ago, enabling the evolution of more complex forms of life (1, 2). Cyanobacteria have colonized most terrestrial environments, thriving even in extreme environment conditions such as high UV light radiation and extreme desiccation (3, 4), representing one of the most morphologically diverse prokaryotic phyla. Traditionally Cyanobacteria have been classified in five different morphological sections: unicellular (section I); unicellular organized in packet-like structures (section II); basic filamentous forms and undifferentiated cells (section III); multicellular and differentiated (section IV); and multicellular and differentiated with the ability to branch in multiple dimensions (section V) (5). Moreover, among cyanobacterial differentiated cells we might find hormogonia (motile cells), akinetes (a kind of spore) and heterocysts (metabolically specialized cells with the ability to fix inorganic nitrogen) (6–8).

Cyanobacteria represent one of the few prokaryotic phyla in which multicellularity evolved. Trait evolution analyses have shown that the earliest linages of Cyanobacteria were unicellular and the emergence of filamentous multicellular representatives occurred very early in the evolution of Cyanobacteria (2, 9–13). Among other characters, such transition required the emergence of a coordinated assembly of cells, cell-to-cell adhesion and intercellular communication leading to a coordinated activity (2, 14–17). In particular, filament formation in Cyanobacteria has been proposed to be the result of gain-of-function mutations (18, 19), and several genes have been reported to be essential for it. For example,

the *fra*C-*fra*D-*fra*E operon and *sep*J (also known as *fra*G) encode for membrane proteins that are needed to produce cell-to-cell joining structures (nanopores) (20, 21) and filament integrity in multicellular heterocyst-forming cyanobacteria (21–29). In the Nostocales, SepJ has three well defined domains: an N-terminal coiled-coil domain, a central linker and a C-terminal permease domain(19, 21); this protein is located at cell poles and it is required for *Anabaena* sp. PCC7120 to form and place nanopores or septal junctions (20, 26), with multimeric SepJ structures at the intercellular septa interacting with peptidoglycan (30, 31). Previous studies have shown molecular exchange between the cytoplasm of cells of filamentous cyanobacteria by using fluorescent tracers, especially calcein (25). Furthermore, calcein-FRAP experiments comparing wild type with *sepJ* null mutants and overexpressors revealed the role of SepJ in mediating intercellular molecular diffusion in *Anabaena* sp. PCC7120 (19, 20, 25).

Other important genes in filament formation such as the cell wall amidases *ami*C1 and *ami*C2 genes are located in tandem in *Nostoc punctiforme* genome and together have also been associated to multicellular phenotypes (32, 33). The protein AmiC1 is required for the correct localization of SepJ at the septum (32), and together they play important role in the placement of nanopores and septal junctions (26) allowing intercellular communication and heterocyst development (32, 33). AmiC2, localized within septa (34) seems to be essential for multicellular development and the filament elongation in *N.punctiforme*, since its knock-out mutant did not grow as a normal filamentous organism but forms clusters of cells that are resistant to disintegration (35). Moreover, a common minimal set of 10 genes has been proposed to be related with filament formation and/or function in Cyanobacteria, including *CyDiv*, *hetR*, *patU3* and *hetZ* (18, 36).

Evolutionary studies have suggested that certain reversions from multi-to-unicellularity occurred within the cyanobacterial phylum (10, 12, 37). One of these cases is represented by the *Gloeocapsa*-like clade, comprised by cyanobacteria that have been traditionally classified in the section II (unicellular cyanobacteria with packet-like phenotypes). The shared ancestry with the filamentous Nostocales clade have suggested that their origin was the result of the loss of some multicellular features(10, 12, 37, 38).

The evolutionary history of *Gloeocapsa*-like cyanobacteria suggests that multicellular phenotypes (e.g., tetrads) commonly observed in unicellular cyanobacteria

from section II (39–41) do not represent random aggregated cells within an extracellular matrix, as previously thought (42–44). Based on their evolutionary origin and morphology (38), we hypothesized that *Gloeocapsa*-like cyanobacteria exhibit an intermediate phenotype, with a phenotypic plasticity that allows it to behave as both multicellular (adhered clusters of cells as multicellular morphotypes) and/or unicellular depending on environmental conditions.

In this work, we studied the extremophile *Gloeocapsopsis* sp. UTEXB3054. By implementing the use of flow cytometry with cell sorting and microscopy, we characterized the phenotypic transitions that *Gloeocapsopsis* sp. UTEX B3054 undergoes during growth in standard liquid medium as well as in modified media. We tested the phylogenomic hypothesis predicting that *Gloeocapsopsis* evolved from the multicellular ancestor shared with the Nostocales. We therefore looked into whether *Gloeocapsopsis* and their close relatives share genes and/or genomic signatures underpinning this reversion. Our comparative genomic analysis revealed that *Gloeocapsopsis* sp. UTEXB3054 retained genomic features previously linked to filamentous multicellularity such as *sep*J, *fra*E, *fra*H and *CyDiv* (all2320), but lacks others such as *ami*C2. Cell-to-cell communication, hallmark of heterocyst-forming cyanobacteria, was confirmed by Calcein-FRAP experiments within multicellular morphotypes of *Gloeocapsopsis.* Our study provides new insights into one of the few reversion events from a multicellular ancestor known to occur in nature. This event gave rise to the unicellular lineage of *Gloeocapsopsis*-like cyanobacteria more than 1.6 billion years ago (10).

Materials and Methods

Strain and culture conditions

Gloeocapsopsis sp. UTEXB3054 was grown in 250 ml Erlenmeyer flasks containing 45 ml of BG11 medium, which is widely used for the cultivation of coccoid cyanobacteria (5, 45). 5 ml aliquots from stationary phase cultures were used to inoculate the medium (Optical Density$_{750}$=1.0). Cultures were incubated at 28ºC without agitation under 10 µE of white light on a 12/12 hour light/dark cycle. Thereafter, OD was measured every two days after gentle manual agitation of the cultures for homogenization. We previously observed that OD_{750} measurements and dry-weight are highly correlated (Pearson correlation r2=0.99; P<0,0001; not shown). OD_{750} was chosen over fluorescence measurements, as pigment per cell may change at the end of culture growth (increasing as self-shading occurs, or sometimes declining as nutrient-limitation occurs), and precise cell counts were complicated by multicellular phenotypes. For studying possible phenotypic changes in cell clusters triggered by environmental stimuli, we modified the BG11 medium. We used BG11 without nitrate (commonly known as $BG11_0$), as well as medium without phosphates. The pH was always adjusted to the same as the replete BG11, and monitored during growth curve. No changes in pH were observed during growth curve in these modified media (data non shown). The inoculation method employed was the same described above. 5 ml aliquots of stationary culture previously grown in replete medium were inoculated in depleted media. The growth curves were performed using cells that have been growing in reduced medium for only one cycle and without washing before inoculation. The rationale behind that was to avoid any type of mechanical disturbance to cell colonies due to washing the culture and to allow the culture undergo growth as it responded to a chemical change in the medium. Growth experiments were performed in 3-4 replicates. For transmission electron microscopy (TEM) and Periodic acid-Schiff staining (PAS)/ Optical microscopy, samples were processed as previously described (46).

Flow cytometry and cell sorting

Samples of *Gloeocapsopsis* sp. UTEXB3054 were analyzed and sorted with an inFlux^{TM} cell sorter (Cytopeia, currently manufactured by BD, Franklin Lakes, NJ, USA). The samples were processed without fixation (see above) immediately after harvesting and

OD measurements. Light scatter and fluorescence were induced with 488-nm and 640-nm excitation lasers (Coherent Inc., Santa Clara, CA, USA). Scatter and fluorescence signals (580-30 nm, phycobiliproteins; 692-40 nm, chlorophyll) were detected with photomultipliers (Hamamatsu Photonics K.K.) and the current pulses were processed with logarithmic amplifiers. Digitized values of pulse heights were recorded with Sortware™ software (BD, Santa Cruz, CA, USA). The instrument was aligned and calibrated with 2 µm YG beads (Polysciences, USA) and 3 µm UltraRainbow fluorescent beads (Spherotech Inc. Libertyville, IL, USA). Alignment was considered satisfactory if the CV of bead singlets was less than 2.5%. The cytometer settings were adjusted to position the peak beads scatter and fluorescence at approximately 90% of the full scale (allowing all cyanobacteria in the cultures to be on-scale). Samples were analyzed, and cells were sorted with a 70 µm ceramic tip at a sample pressure of 1-2 psi above the sheath pressure (15 psi). Cells were run a rate of 2000 cells/s. Fluorescence and scatter profiles were obtained by running samples for 2 minutes. For sorting the instrument was loaded with a sterile sheath fluid of 3% NaCl, that was sterilized by filtration through a 0.2 µm filter. A Sterivex filter mounted in the sheath line of the system served as a second filtration stage. Sorting of selected scatter and fluorescence regions was performed using 1-drop purity mode. Flow cytometry profiles were analyzed using FlowJo Software.

Comparative Genomic Analyses

A genomic screening was conducted in order to identify multicellular related genes in unicellular and multicellular cyanobacterial genomes. Amino acid sequences from proteins functionally characterized in *Anabaena* sp. PCC7120 were downloaded from the IMG/JGI database and used for tBLASTn (47) comparison searches (thresholds used: e-value $<10^{-25}$ and bit score >100) in other cyanobacterial genomes downloaded from same database. Code accession of cyanobacterial genomes and amino acid sequences are found in Supplementary Information Table S1.

Phylogenetic Analyses

All sequence data were obtained from GenBank (www.ncbi.nlm.nih.gov). A total of 350 cyanobacterial genomes were screened (Table S2) using *Anabaena*'s SepJ sequence as query. Gene sequences were aligned using MAFFT v7.123b (48). To investigate the

evolution of SepJ, we performed phylogenetic analyses based on the C-terminal permease domain, conserved among homologue sequences found (this section includes the last 339 aa from the protein alignment found in Fig. S1). Bayesian analyses were implemented to determine the phylogenetic relationships of SepJ under the CAT-GTR+G model in Phylobayes MPI 1.7a (49). Convergence of Bayesian analyses was tested using the software Tracecomp (in Phylobayes). In order to know position of the root in the tree, different rooting options were evaluated by implementing different methodologies: (1) outgroup rooting (50, 51), (2) midpoint rooting (52), and (3) Bayesian molecular clock rooting (53). We used *Pseudanabaena* SepJ for outgroup rooting. The midpoint rooting was estimated in R (54), and the root that minimizes the variance of root-to-tip distances was estimated in TempEst v1.5.1 (55).

Calcein loading

Calcein is a hydrophilic molecule of 623 Da, which can be loaded into cyanobacterial cells as the cell-permeant acetoxymethyl ester derivative (25). Esterase activity in the cytoplasm releases a fluorescent product that is trapped in the cytoplasm because it is too hydrophilic to diffuse across lipid bilayers. Intercellular exchange of calcein has been monitored by confocal fluorescence recovery after photobleaching (FRAP) experiments in which fluorescence is bleached in one cell (e.g. of a filament). Subsequent imaging can reveal re-equilibration of fluorescent calcein between cells due to simple diffusion through septal junctions: protein channels which link the cytoplasm of adjacent cells in the filament (25, 56, 57). In this study, calcein was loaded into the cytoplasm of *Gloeocapsopsis* cells using a protocol adapted from Mullineaux et al., 2008 (25). The acetoxymethyl ester derivative of calcein (Calcein AM; Thermo Fisher Scientific) was dissolved in dimethylsulfoxide to a concentration of 1mg/ml. 0.5 ml of cell culture was harvested by gentle centrifugation, washed twice in fresh BG11 medium, resuspended in 0.5 ml fresh medium and mixed with 10 µl calcein AM solution. The cells were then incubated in the dark at 28 °C for 90 min before harvesting and washing 3 times in fresh BG11 medium. Small drops of cell suspension were spotted onto BG11 agar plates and incubated until all the free liquid was evaporated or adsorbed. Blocks of agar with the cells on the surface were cut from the plate, placed on a cover-slip and mounted in the well of a

229 custom-built sample holder.

230 *Confocal microscopy and Fluorescence Recovery After Photobleaching*

231 Cells were imaged with a Leica TCS SP5 laser scanning confocal microscope with
232 63X oil-immersion objective lens (numerical aperture 1.4). The confocal pinhole was set to
233 give a resolution in the *z*-direction of approximately 8 µm. Excitation was with the 488 nm
234 line of an argon laser. Monochromators were set to image calcein fluorescence at 503-515
235 nm and chlorophyll fluorescence at 670-720 nm. Bleaching was accomplished by a single
236 scan over a box of 3.8 x 3.8 µm overlapping with one cell in the field of view.
237
238 **Results**
239 *Morphology and ultrastructure of* Gloeocapsopsis
240 In nature and also when growing in liquid medium, *Gloeocapsopsis* sp. UTEX
241 B3054 appears both as single cells and forming cellular packets or clusters containing
242 between 2 and 4 cells, or even more cells (Fig. 1). Ultrastructural observations showed that
243 the EPS is concentrically organized around cells in an onion-like configuration throughout
244 the growth of *Gloeocapsopsis* sp. UTEX B3054. Clustered cells tend to be attached by
245 sugar-rich extracellular matrix (Fig. 1A) that shows blue autofluorescence (Fig. 1B),
246 forming the archetypal tetrads and packet-like clusters with multiple cells observed in
247 nature (Figs. 1C, 1E, 1F) (hereafter termed colonies and/or multicellular phenotypes). Each
248 cell is delimited by the cell wall structure typical of cyanobacteria, which is comprised by
249 the cytoplasmic membrane (CM), a peptidoglycan layer (Pg) and the outer membrane (OM)
250 (Fig. 1D). The periplasmic space between the peptidoglycan and the outer membrane was
251 not continuous among cells. Cell division occurs through equal binary fission within the
252 EPS (Fig. 1E).
253 *Changes of cellular morphotypes during growth*
254 Based on the autofluorescence of *Gloeocapsopsis* phenotypes (determined by light
255 harvesting pigments such as chlorophyll, phycocyanin and phycoerythrin) and light
256 scattering signatures of cells, flow cytometry coupled to particle sorting allowed us to
257 distinguish between single cells of *Gloeocapsopsis* sp. UTEXB3054 and its several
258 (multi)cellular phenotypes. Three main phenotypic groups of *Gloeocapsopsis* were defined
259 for further analysis: (a) single cells, (b) groups of intermediate colonies (primarily

phenotypes comprising between 2 and 4 cells) and (c) colonies with more than 4 cells (multiple or multicellular clusters) (Fig. S2). Noteworthy, single cell phenotypes (cells with the lowest light scatter signals) included two different groups of cells in terms of red (692-40 nm) and orange (580-30 nm) fluorescence when excited with blue light (488 nm) (Fig. S3). Analysis of both single cell phenotypes using the violet laser (405 nm) indicated that some of them lacked blue autofluorescence, whereas all the other *Gloeocapsopsis*'s phenotypes presented blue autofluorescence (data non shown).

The culture exhibited a consistent pattern of changes in intercellular organization during growth under replete conditions, with the highest levels of phenotypic heterogeneity occurring under active growth phase (Figs. 2 and 3). At this stage, red-fluorescent single cells significantly increased up to 20% of the total phenotypes, tending to disappear when entering into stationary phase (Table S3). Once in active growth, cellular phenotypes with intermediate light scattering properties split into two main subgroups with different light scattering properties, turning back into the distribution observed in lag-phase and early growth once in stationary phase (Fig. 3). Finally, the presence of multicellular phenotypes significantly increased under active growth (Fig. 2 and Table S3), turning back to original values once in stationary phase (Fig. 2 and Table S3).

The morphotypes exhibited by *Gloeocapsopsis* sp. UTEX B3054 changed when the chemical composition of the medium was modified (Fig. 2; dashed lines). In contrast to what was observed under replete growth, light scattering signatures of phosphate-deprived cultures were more homogeneous during the active phase of growth (Fig. 2C-D). The intermediate colonies were more prevalent in phosphate-deprived medium in comparison to standard medium, while the presence of multicellular colonies was significantly lower (Tables S3 and S4). Moreover, the orange-fluorescent single cell phenotype almost disappeared during active and stationary growth under phosphate-limited conditions (Tables S3 and S4). The intrinsic ability of *Gloeocapsopsis* to organize in different multicellular morphotypes was less affected under nitrate-deprivation ($BG11_0$ medium) (Tables S3 and S4). However, in $BG11_0$ medium there was a significant decrease in the proportion of intermediate colonies during active growth, while there was an increase in the proportion of red-fluorescent single cells during both active growth and stationary phase. The differences observed in terms of the ability to form different phenotypes under

different growth media were not reflected in biomass change measured by light transmittance correlated to differences in biomass increase of the cultures (data non shown).

Comparative genomic analyses for key genes associated with multicellularity.

The organized phenotypic transitions observed during *Gloeocapsopsis* growth and its ability to modify the patterned growth under different chemical settings in media lead us to predict that *Gloeocapsopsis* and its close relatives likely retained some multicellular features which might be found in their genomes.

Based on genes functionally associated with multicellular abilities in Cyanobacteria, we performed a genomic survey in cyanobacterial genomes. Homologues of all multicellular related genes (18) were found in Nostocales genomes but were absent in model unicellular cyanobacteria such as *Prochlorococcus* and *Synechoccocus* (Table 1). Noteworthy, Chrooccacceae cyanobacteria encode for some of them, including homologous genes of *fra*E and *fra*H (Table 1). For instance, homologous genes of the well-described *Anabaena*'s *fra*-operon were conserved in all the Nostocales cyanobacteria, although only some isolated homologous genes were present in Chroooccacceae genomes, which lack of *fra*C and *fra*D. The cell wall amidase genes *ami*C1 and *ami*C2 occurring in tandem were found to be exclusive of Nostocales cyanobacteria (Fig. 4). In contrast to Nostocales, we found that Chroococccacceae cyanobacteria only possess *ami*C1, lacking the adjacent gene copy of the multicellular-related amidase gene (*ami*C2). However, *ami*C1 in Chroococccacceae occurred in a conserved genomic context to the Nostocales *ami*C1 and *ami*C2, being upstream and same orientation as a glutamate racemase (COG0796), transnonapredyl diphosphate synthase (COG0142) and a transglutaminase-like putative cysteine protease (COG1305) (Fig. 4).

Phylogeny of SepJ

A blast search using the functionally described SepJ aminoacid sequence of *Anabaena* sp. PCC7120 showed that 179 of the 350 cyanobacterial genomes screened encode an homologue sequence of SepJ. Strictly unicellular cyanobacteria like *Synechoccoccus* and *Prochlorococcus* lack SepJ-like sequences. All Chroococcacceae cyanobacteria encode for a partial or shorter homologue to *Anabaena*'s SepJ: a Drug/Metabolite Exporter (DME)-family permease, with high levels of amino acid identity (34% of sequence identity and

53% of positive substitutions), lacking both the N-terminal domain with the predicted coiled-coil domain (CC) and the internal linker region (L) characteristics of the *Anabaena*'s SepJ (Table S5 and Figure S1). Bayesian phylogenetic analysis of SepJ and DME-family permease homologues found in 179 cyanobacterial genomes show that they are sister clades (Fig. 5). Within the DME-family permease clade there are some well-defined groups including Nostocales, and some cyanobacteria traditionally classified as unicellular (e.g. *Gloeocapsopsis*, *Chroococcidiopsis*). Within the SepJ clade, we found SepJ-like proteins comprised by two or three domains (CC+P; CC+L+P). The SepJ topology is consistent with previously published genome phylogenies (10) (Fig. 5; see also Fig. S4 to statistical support and posterior probabilities). Possible topology rooting options explored are illustrated in an unrooted topology (Fig. S5). SepJ variants shows that the *Pseudanabaena*-like homologue to SepJ is basal, followed by a paraphyletic group containing filamentous cyanobacteria that do not undergo any cell differentiation (e.g. *Phormidium, Oscilatoria, Leptolyngbya)* and a more recently divergent group including the Nostocales SepJ. DME-family permease sequences are found in both filamentous cyanobacteria (e.g. *Nostoc* and *Leptolyngbya*, among others) and cluster-forming unicellular cyanobacteria (e.g. *Chroococcidiopsis, Acaryochloris).* Interestingly, 56,7% of DME-family permeases are encoded by taxa that do also encode for long SepJ variants (*Nostoc* and *Leptolyngbya*, among others) (Table S5).

Cell-to-cell communication

We tested for the possibility of intercellular communication in dyads and tetrads of *Gloeocapsopis* by performing calcein FRAP experiments. We found that calcein could be loaded into the cytoplasm of *Gloeocapsopsis* similarly to *Anabaena*. However, in *Gloeocapsopsis* culture only a minority of cells was successfully loaded, most probably due to the thick capsule of EPS. FRAP experiments conducted by bleaching one cell in a calcein-loaded dyad or tetrad revealed slow intercellular exchange of calcein, even when cell division appeared complete as judged from bright-field and chlorophyll fluorescence images.

Representative examples of cell-to-cell communication in dyads and tetrads are shown in Fig. 6 and Fig. S6. Calcein exchange was not detected in every case, and it occurs

352 on a slow timescale of up to a few minutes, in contrast to the faster exchange described in
353 *Anabaena* (25).
354
355 **Discussion**
356 Our microscopical observations indicate that *Gloeocapsopsis* cells are not randomly
357 aggregated but are organized within an extracellular matrix exhibiting an onion-like
358 structure, with the outermost EPS layer surrounding all the cells. Moreover, during active
359 growth *Gloeocapsopsis* exhibit different cellular groups corresponding to phenotypic
360 transitions, including single cells, intermediate colonies and multicellular colonies with
361 more than four cells. Although neither cell-to-cell adhesions nor membrane contact
362 between cells were observed in any of the ultrathin cuts, this cyanobacterium showed an
363 intrinsic ability to form adhered clusters of cells (multicellular phenotypes) depending on
364 growth stage and/or environmental changes. When growth is limited, *Gloeocapsopsis* sp.
365 UTEX B3054 cells arrest in dyads, triads, or tetrads, while in active growth the organism
366 appears to cycle also through single-cell stages. Our results of microscopy and flow
367 cytometry support the notion that this cyanobacterium displays a facultative or transient
368 multicellularity that might be induced in response to environmental cues.
369 Recent genomic data have improved the resolution of the Cyanobacteria phylogeny
370 (10, 12, 37). Evolutionary studies suggest that some unicellular cyanobacteria evolved from
371 a multicellular ancestor, and our comparative genomic analyses unveiled several genomic
372 signatures likely involved in the loss of multicellularity leading to origin the *Gloeocapsa*-
373 like clade. Our results suggest that the organization of multicellular phenotypes observed in
374 *Gloeocapsopsis* sp. UTEX B3054 might be reflected at the genomic level. *Gloeocapsa*-like
375 cyanobacteria do not encode homologous genes of *fra*C and *fra*D, needed for the calcein
376 transfer pathway to be operative in *Anabaena* (27) by gating the septal junctions (26).
377 However, other genes associated to filament integrity in *Anabaena* such as *fra*E and *fra*H
378 (27, 58, 59) were found in the genome of *Gloeocapsopsis* and its close relatives. Two cell
379 wall amidase genes *ami*C1 and *ami*C2 occurring in tandem in a preserved genomic context
380 due to a gene duplication event (60) seems to be an exclusive feature of Nostocales.
381 However, while the *Gloeocapsa*-like clade lacks *ami*C2, the genomic context is highly
382 conserved. Genetic studies have shown that *ami*C2 mutants in the Nostocales affect

processing of septal peptidoglycan (the PG is fully split between neighboring cells in cell groups), leading to less invaginated murein sacculus when comparing to wild-type cells (35). The overall morphology of *ami*C2 mutant in the Nostocales described in Lehner et al. (2011) is somewhat similar to *Gloeocapsopsis* wild type described in this work (Fig.1E). It seems that this gene duplication was a key innovation associated to the emergence of diazotrophic filament-forming multicellular cyanobacteria.

SepJ has been described as a crucial protein during the formation of the multicellular septum in filamentous cyanobacteria (19–21, 25, 30, 61). Our phylogenetic analyses and rooting of SepJ and DME-family permease show that these two homologues likely arose by gene duplication in a common ancestor prior to the divergence of *Pseudanabaena.* Within the SepJ clade, the branching of an early basal lineage of *Pseudanabaena*-like SepJ is consistent with previous phylogenomic and trait evolution studies showing that *Pseudoanabaena* filamentous forms evolve early on in Cyanobacteria (1, 2, 10, 12, 13, 62). The topology of SepJ is consistent with previously published genome phylogenies showing the Nostocales as the most recently derived group of filamentous cyanobacteria (10). SepJ and DME-permease evolved near the root of Cyanobacteria. SepJ variants are only found in filamentous forms, and they must be the result of a series of gain-of-function mutations, by which the protein gradually acquired the coil-coiled and the linker domain and therefore, new functions (19). The permease domain represents the integral membrane section of the protein and has been demonstrated to be necessary for the formation of the septum junctions between cells, to participate in the intercellular communication, as well as to allow proper filament elongation in diazotrophic filamentous cyanobacteria (19–21, 23, 25, 30, 56, 63, 64). Due to the absence of direct cell-to-cell contact in *Gloeocapsopsis* as well as the lack of diazotrophic functions, we hypothesize that DME-permease participate in transport processes associated to intercellular communication.

Our calcein-FRAP results confirm that *Gloeocapsopsis* cells carry out cell-to-cell communication, previously considered a hallmark of differentiated multicellular cyanobacteria (57). The results are consistent with a limited cell-to-cell communication activity observed within *Gloeocapsopsis* dyads and tetrads. Such limited activity could allow the intercellular diffusion of metabolites and signaling molecules, as it does in

filamentous cyanobacteria. We further hypothesize that some of the traditionally classified unicellular cyanobacteria encoding for DME-family permease might be able to carry out a still unknown mechanism of cell-to-cell communication; this could be further tested with an experimental approach.

We propose that *Gloeocapsopsis* is not a strictly unicellular cyanobacterium but a facultative multicellular organism, a biological condition that might be ecologically advantageous at some stages of their life cycle or under certain environmental conditions such as desiccation. If cells were highly connected, the likelihood of a catastrophic drying for the whole cell cluster would greatly increase. Therefore, a transient multicellularity with low levels of cell-to-cell communication may be crucial providing a limited buffering of water and solute concentrations among cells, which may contribute for allowing these organisms to thrive in extreme conditions such as those found in the Atacama Desert. Phenotypic transitions may have evolved for mitigating some stresses (i.e., nutrient or water shortage). Further research using environmentally realistic changes in nutrients and water availability will help to clarify this hypothesis.

Acknowledgments

We thank Alejandro Munizaga (UMA-BIO) for technical support with samples preparation for the TEM Microscope, and Giorgio Bianchini for technical assistance with the analyses of SepJ. Phylogenetic analyses were performed at the High-Performance Computer facility (BlueCrystal 4) at the University of Bristol. Funding support for PS-B came from a Royal Society University Research Fellowship. LS and RV were partially supported by grants from FONDECYT (1110597) and the Millennium Institute for Fundamental and Applied Biology (MIFAB). CU was funded by the doctoral fellowship from CONICYT and also by Beca Gastos Operacionales CONICYT 21110394. Funding support for PvD came from Instituto Milenio de Oceanografía. The Influx cell sorter was purchased with FONDEQUIP EQM130267.

Author contributions

CU, PvD, RV and PS-B designed the research. CU and GvE isolated the strain by cell sorting. CU and LS maintained and prepared cultures for experiments. LS performed growth curves experiments. CU, PvD, GvE performed flow cytometry experiments and analyses. CU performed comparative genomic analyses under the guidance of PS-B. PS-B performed the phylogenomic analyses of SepJ. CM performed FRAP experiments and analyses. CU, PvD, CM, RV and PS-B wrote the manuscript. All co-authors have read and contributed to the final version of the manuscript.

Competing interests

All authors declare no competing interests.

References

1. Schirrmeister BE, Gugger M, Donoghue PCJ. 2015. Cyanobacteria and the Great Oxidation Event: evidence from genes and fossils. Palaeontology 58:769–785.
2. Schirrmeister BE, de Vos JM, Antonelli A, Bagheri HC. 2013. Evolution of multicellularity coincided with increased diversification of cyanobacteria and the Great Oxidation Event. Proc Natl Acad Sci U S A 110:1791–1796.
3. Potts M. 1999. Mechanisms of desiccation tolerance in cyanobacteria. Eur J Phycol 34:319–328.
4. Billi D, Baqué M, Smith HD, Mckay CP. 2013. Cyanobacteria from extreme deserts to space. Adv Microbiol 2013:80–86.
5. Rippka R, Deruelles J, Waterbury JB, Herdman M, Stanier R. 1979. Generic assignments, strain histories and properties of pure cultures of cyanobacteria. J Gen Microbiol 110:1–61.
6. Herdman M, Rippka R. 1988. Cellular differentiation: hormogonia and baeocytes, p. 232–242. *In* Methods in Enzymology.
7. Meeks JC, Campbell EL, Summers ML, Wong FC. 2002. Cellular differentiation in the cyanobacterium Nostoc punctiforme. Arch Microbiol 178:395–403.
8. Adams DG. 2000. Heterocyst formation in cyanobacteria. Curr Opin Microbiol 3:618–624.
9. Blank CE, Sanchez-Baracaldo P. 2010. Timing of morphological and ecological innovations in the cyanobacteria - A key to understanding the rise in atmospheric oxygen. Geobiology 8:1–23.
10. Sánchez-Baracaldo P. 2015. Origin of marine planktonic cyanobacteria. Sci Rep 5:17418.
11. Garcia-Pichel F, Lombard J, Soule T, Dunaj S, Wu SH, Wojciechowski MF. 2019. Timing the evolutionary advent of cyanobacteria and the later great oxidation event using gene phylogenies of a sunscreen. MBio 10:1–14.
12. Schirrmeister BE, Antonelli A, Bagheri HC. 2011. The origin of multicellularity in cyanobacteria. BMC Evol Biol 11:45.
13. Schirrmeister BE, Sanchez-Baracaldo P, Wacey D. 2016. Cyanobacterial evolution during the Precambrian. Int J Astrobiol 1–18.
14. Flores E, Herrero A. 2010. Compartmentalized function through cell differentiation in filamentous cyanobacteria. Nat Rev Microbiol 8:39–50.
15. Herrero A, Stavans J, Flores E. 2016. The multicellular nature of filamentous heterocyst-forming cyanobacteria. FEMS Microbiol Rev 40:831–854.
16. Claessen D, Rozen DE, Kuipers OP, Søgaard-Andersen L, van Wezel GP. 2014. Bacterial solutions to multicellularity: a tale of biofilms, filaments and fruiting bodies. Nat Rev Microbiol 12:115–124.
17. Lyons NA, Kolter R. 2015. On the evolution of bacterial multicellularity. Curr Opin Microbiol 24:21–28.
18. Stucken K, John U, Cembella A, Murillo AA, Soto-Liebe K, Fuentes-Valdés JJ, Friedel M, Plominsky AM, Vásquez M, Glöckner G. 2010. The smallest known

genomes of multicellular and toxic cyanobacteria: comparison, minimal gene sets for linked traits and the evolutionary implications. PLoS One 5:e9235.

19. Mariscal V, Herrero A, Nenninger A, Mullineaux CW, Flores E. 2011. Functional dissection of the three-domain SepJ protein joining the cells in cyanobacterial trichomes. Mol Microbiol 79:1077–1088.

20. Mariscal V, Nürnberg DJ, Herrero A, Mullineaux CW, Flores E. 2016. Overexpression of SepJ alters septal morphology and heterocyst pattern regulated by diffusible signals in Anabaena. Mol Microbiol 101:968–981.

21. Flores E, Pernil R, Muro-Pastor AM, Mariscal V, Maldener I, Lechno-Yossef S, Fan Q, Wolk CP, Herrero A. 2007. Septum-localized protein required for filament integrity and diazotrophy in the heterocyst-forming cyanobacterium Anabaena sp. strain PCC 7120. J Bacteriol 189:3884–3890.

22. Merino-Puerto V, Schwarz H, Maldener I, Mariscal V, Mullineaux CW, Herrero A, Flores E. 2011. FraC/FraD-dependent intercellular molecular exchange in the filaments of a heterocyst-forming cyanobacterium, Anabaena sp. Mol Microbiol 82:87–98.

23. Nürnberg DJ, Mariscal V, Bornikoel J, Nieves-Morión M, Krauss N, Herrero A, Maldener I, Flores E, Mullineaux CW. 2015. Intercellular diffusion of a fluorescent sucrose analog via the septal junctions in a filamentous cyanobacterium. MBio 6:1–12.

24. Omairi-Nasser A, Mariscal V, Austin JR, Haselkorn R. 2015. Requirement of Fra proteins for communication channels between cells in the filamentous nitrogen-fixing cyanobacterium Anabaena sp. PCC 7120. Proc Natl Acad Sci U S A 112:E4458–E4464.

25. Mullineaux CW, Mariscal V, Nenninger A, Khanum H, Herrero A, Flores E, Adams DG. 2008. Mechanism of intercellular molecular exchange in heterocyst-forming cyanobacteria. EMBO J 27:1299–1308.

26. Weiss GL, Kieninger A-K, Maldener I, Forchhammer K, Pilhofer M. 2019. Structure and function of a bacterial gap junction analog. Cell 178:374–384.

27. Merino-Puerto V, Mariscal V, Mullineaux C, Herrero A, Flores E. 2010. Fra proteins influencing filament integrity , diazotrophy and localization of septal protein SepJ in the heterocyst-forming cyanobacterium Anabaena sp . Mol Microbiol 75:1159–1170.

28. Wilk L, Strauss M, Rudolf M, Nicolaisen K, Flores E, Kühlbrandt W, Schleiff E. 2011. Outer membrane continuity and septosome formation between vegetative cells in the filaments of Anabaena sp. PCC 7120. Cell Microbiol 13:1744–54.

29. Nayar AS, Yamaura H, Rajagopalan R, Risser DD, Callahan SM. 2007. FraG is necessary for filament integrity and heterocyst maturation in the cyanobacterium Anabaena sp. strain PCC 7120. Microbiology 153:601–607.

30. Ramos-León F, Mariscal V, Battchikova N, Aro EM, Flores E. 2017. Septal protein SepJ from the heterocyst-forming cyanobacterium Anabaena forms multimers and interacts with peptidoglycan. FEBS Open Bio 7:1515–1526.

31. Ramos-Leon F, Mariscal V, Frias JE, Flores E, Herrero A. 2015. Divisome-dependent subcellular localization of cell-cell joining protein SepJ in the filamentous cyanobacterium Anabaena. Mol Microbiol 96:566–580.

32. Bornikoel J, Carrión A, Fan Q, Flores E, Forchhammer K, Mariscal V, Mullineaux CW, Perez R, Silber N, Wolk CP, Maldener I. 2017. Role of Two Cell Wall Amidases in Septal Junction and Nanopore Formation in the Multicellular

Cyanobacterium Anabaena sp. PCC 7120. Front Cell Infect Microbiol 7:1–15.
33. Berendt S, Lehner J, Zhang YV, Rasse TM, Forchhammer K, Maldener I. 2012. Cell wall amidase amic1 is required for cellular communication and heterocyst development in the cyanobacterium Anabaena PCC 7120 but not for filament integrity. J Bacteriol 194:5218–5227.
34. Büttner FM, Faulhaber K, Forchhammer K, Maldener I, Stehle T. 2016. Enabling cell-cell communication via nanopore formation: Structure, function and localization of the unique cell wall amidase AmiC2 of Nostoc punctiforme. FEBS J 283:1336–1350.
35. Lehner J, Zhang Y, Berendt S, Rasse TM, Forchhammer K, Maldener I. 2011. The morphogene AmiC2 is pivotal for multicellular development in the cyanobacterium Nostoc punctiforme 79:1655–1669.
36. Mandakovic D, Trigo C, Andrade D, Riquelme B, Gómez-Lillo G, Soto-Liebe K, Díez B, Vásquez M. 2016. CyDiv, a Conserved and Novel Filamentous Cyanobacterial Cell Division Protein Involved in Septum Localization. Front Microbiol 7:1–11.
37. Shih PM, Wu D, Latifi A, Axen SD, Fewer DP, Talla E, Calteau A, Cai F, Tandeau de Marsac N, Rippka R, Herdman M, Sivonen K, Coursin T, Laurent T, Goodwin L, Nolan M, Davenport KW, Han CS, Rubin EM, Eisen JA, Woyke T, Gugger M, Kerfeld CA. 2013. Improving the coverage of the cyanobacterial phylum using diversity-driven genome sequencing. Proc Natl Acad Sci U S A 110:1053–1059.
38. Urrejola C, Alcorta J, Salas L, Vásquez M, Polz MF, Vicuña R, Díez B. 2019. Genomic features for desiccation tolerance and sugar biosynthesis in the extremophile Gloeocapsopsis sp. UTEX B3054. Front Microbiol 10:1–11.
39. de los Ríos A, Valea S, Ascaso C, Davila A, Kastovsky J, Mckay CP, Gómez-Silva B, Wierzchos J. 2010. Comparative analysis of the microbial communities inhabiting halite evaporites of the Atacama Desert. Int Microbiol 13:79–89.
40. Wierzchos J, Davila AF, Artieda O, Cámara-Gallego B, de los Ríos A, Nealson KH, Valea S, Teresa García-González M, Ascaso C. 2012. Ignimbrite as a substrate for endolithic life in the hyper-arid Atacama Desert: Implications for the search for life on Mars. Icarus 224:334–346.
41. Roldán M, Ascaso C, Wierzchos J. 2014. Fluorescent fingerprints of endolithic phototrophic cyanobacteria living within halite rocks in the Atacama Desert. Appl Environ Microbiol 80:2998–3006.
42. Waterbury JB, Stanier RY. 1978. Patterns of growth and development in Pleurocapsalean cyanobacteria. Microbiol Rev 42:2–44.
43. Ramos V, Seabra R, Brito Â, Santos A, Santos CL, Lopo M, Moradas-Ferreira P, Vasconcelos VM, Tamagnini P. 2010. Characterization of an intertidal cyanobacterium that constitutes a separate clade together with thermophilic strains. Eur J Phycol 45:394–403.
44. Cumbers J, Rothschild LJ. 2014. Salt tolerance and polyphyly in the cyanobacterium Chroococcidiopsis (Pleurocapsales). J Phycol 50:472–482.
45. Stanier RY, Kunisawa R, Mandel M, Cohen-Bazire G. 1971. Purification and properties of unicellular blue-green algae (order Chroococcales). Bacteriol Rev 35:171–205.
46. Azúa-Bustos A, Zúñiga J, Arenas-Fajardo C, Orellana M, Salas L, Vicuña R. 2014. Gloeocapsopsis AAB1, an extremely desiccation-tolerant cyanobacterium isolated

from the Atacama Desert. Extremophiles 18:61–74.
47. Altschul SF, Madden TL, Schäffer A, Zhang J, Zhang Z, Miller W, Lipman DJ. 1997. Gapped BLAST and PSI-BLAST: a new generation of protein database search programs. Nucleic Acids Res 25:3389–3402.
48. Katoh K, Standley DM. 2013. MAFFT multiple sequence alignment software version 7: Improvements in performance and usability. Mol Biol Evol 30:772–780.
49. Lartillot N, Rodrigue N, Stubbs D, Richer J. 2013. PhyloBayes MPI: Phylogenetic reconstruction with infinite mixtures of profiles in a parallel environment. Syst Biol 62:611–615.
50. Wheeler WC. 1990. Nucleic Acid Sequence Phylogeny and Random Outgroups. Cladistics 6:363–367.
51. Boykin LM, Kubatko LS, Lowrey TK. 2010. Comparison of methods for rooting phylogenetic trees: A case study using Orcuttieae (Poaceae: Chloridoideae). Mol Phylogenet Evol 54:687–700.
52. Swofford DL, Olsen GJ, Waddell PJ, Hillis DM. 1996. Phylogenetic inference, p. 407–514. *In* Hillis, DM, Moritz, D, Mable, BK (eds.), Molecular Systematics. Sinauer Associates, Sunderland (MA).
53. Huelsenbeck JP, Bollback JP, Levine AM. 2002. Inferring the root of a phylogenetic tree. Syst Biol 51:32–43.
54. Schliep KP. 2011. phangorn: Phylogenetic analysis in R. Bioinformatics 27:592–593.
55. Rambaut A, Lam TT, Max Carvalho L, Pybus OG. 2016. Exploring the temporal structure of heterochronous sequences using TempEst (formerly Path-O-Gen). Virus Evol 2:vew007.
56. Nieves-Morión M, Mullineaux CW, Flores E. 2017. Molecular diffusion through cyanobacterial septal junctions. MBio 8:1–5.
57. Flores E, Nieves-Morión M, Mullineaux C. 2019. Cyanobacterial Septal Junctions: Properties and Regulation. Life 9:1.
58. Bauer CC, Buikema WJ, Black K, Haselkorn R. 1995. A short-filament mutant of Anabaena sp. strain PCC 7120 that fragments in nitrogen-deficient medium. J Bacteriol 177:1520–1526.
59. Merino-Puerto V, Mariscal V, Schwarz H, Maldener I, Mullineaux CW, Herrero A, Flores E. 2011. FraH is required for reorganization of intracellular membranes during heterocyst differentiation in Anabaena sp. strain PCC 7120. J Bacteriol 193:6815–6823.
60. Koch R, Kupczok A, Stucken K, Ilhan J, Hammerschmidt K, Dagan T. 2017. Plasticity first : molecular signatures of a complex morphological trait in filamentous cyanobacteria 1–11.
61. Escudero L, Mariscal V, Flores E. 2015. Functional dependence between septal protein SepJ from Anabaena sp. Strain PCC 7120 and an amino acid ABC-type uptake transporter. J Bacteriol 197:2721–2730.
62. Schirrmeister BE, Anisimova M, Antonelli A, Bagheri HC. 2011. Evolution of cyanobacterial morphotypes: taxa required for improved phylogenomic approaches. Commun Integr Biol 4:424–7.
63. Flores E, Herrero A, Forchhammer K, Maldener I. 2016. Septal Junctions in Filamentous Heterocyst-Forming Cyanobacteria. Trends Microbiol 24:79–82.
64. Ramos-León F, Arévalo S, Mariscal V, Flores E. 2018. Specific mutations in the

633 permease domain of septal protein SepJ differentially affect functions related to
634 multicellularity in the filamentous cyanobacterium Anabaena. Microb Cell 5:555–
635 565.
636

637 **Figure Legends**

638 **Figure 1.** Morphology and general cellular features of *Gloeocapsopsis* sp. UTEX B3054.
639 **(A)** Periodic acid-Schiff stained cells of *Gloeocapsopsis* sp. UTEX B3054. PAS staining
640 reveals sugar presence in both the EPS and the intracellular space. Scale bar: 4.0 µm. **(B)**
641 Blue autofluorescence in extracellular polymer substances of *Gloeocapsopsis* sp. UTEX
642 B3054. Scale bar: 3.5 µm. **(C)** Transmission electron photomicrograph of a characteristic
643 tetrad during the exponential phase of growth. EPS envelopes surround cells and a laminar
644 sheath is clearly distinguished enclosing only two cells. The thylakoid network is localized
645 at the cytoplasmic periphery. Scale bar: 950 nm. **(D)** Detail of photomicrograph shown in
646 (C). The cell wall is constituted by: the cytoplasmic membrane (CM), peptidoglycan (Pg)
647 and the outer membrane (OM). Scale bar: 173 nm **(E)** Cell division. Cs indicates presence
648 of carboxysome. Black arrow points to the division ring. Scale bar: 600 nm. **(F)**
649 Transmission electron photomicrograph of a multicellular colony, whose cells are
650 maintained together by the outermost sheath. Scale bar: 1.2 µm.
651
652 **Figure 2.** Effect of culturing media on *Gloeocapsopsis*'s phenotypes during growth.
653 Histograms of FSC (**A, C, E**) and red fluorescence (**B, D, F**) for *Gloeocapsopsis* sp. UTEX
654 B3054. Different nutritional conditions are indicated with different line types. Replete
655 BG11 (thick solid line); nitrate-deprived culture (dotted line); and phosphate-deprived
656 culture (dashed line). Note that in these and subsequent figures, a representative replica of
657 each different nutritional treatment is shown. The frequency distribution was normalized to
658 mode. Panels (**A), (B)** represent *Gloeocapsopsis*'s population distribution at early growth (3
659 days after inoculation; OD = 0.1); (**C), (D)** represent *Gloeocapsopsis*'s population
660 distribution at mid active growth phase (8 days after inoculation; OD = 0.5) and panels (**E),**
661 **(F)** represent *Gloeocapsopsis*'s population distribution at stationary growth phase (15 days
662 after inoculation).
663
664 **Figure 3.** Intermediate phenotypes change once reaching the active phase of growth.
665 *Gloeocapsopsis* sp. UTEX B3054 population experimented dynamic changes throughout
666 time. (A), (B) and (C) Early, active and stationary phase, respectively. The initial
667 intermediate phenotypic group splits into two main subgroups once in the active phase

(shown with arrows in B). Note that in these and subsequent flow cytometry figures, only a representative replica is shown. Beads are shown as reference.

Table 1. Multicellular related genes in cyanobacterial genomes

Figure 4. *Gloeocapsopsis* sp. UTEXB3054 and its relatives are naturally-occuring knock-outs of *ami*C2.

Genomic organization of *ami*C1 and *ami*C2 in *S.elongatus* PCC6301, *Nostoc* sp. PCC7107, *Nostoc* sp. PCC7524, *Nostoc azzollae* 0708, *Fischerella* sp. PCC 9605, *Calothrix* sp. PCC 6303, *C.thermalis* PCC7203, *Gloeocapsa* sp. PCC7428 and *Gloeocapsopsis* sp. UTEX B3054. Genes shared are shown in color. *ami*C1 is conserved in all genomes, as well as a glutamate racemase upstream, and a transnonpredyl dipshophate synthase and a transglutaminase like putative cysteine protease downstream. In Nostocales, *ami*C2 was gained likely by a gene duplication of *ami*C1. *Gloeocapsa*-like cyanobacteria lack *ami*C2 in this genomic vicinity, preserving a glutamate racemase and a transnonapredyl diphosphate synthase downstream.

Figure 5. Evolution of SepJ in Cyanobacteria.

The Bayesian phylogenetic tree shown was estimated based on 171 SepJ sequences. Analyses were performed under the CAT-GTR+G model in Phylobayes MPI 1.7a (49). The topology was simplified to show the main clades of both DME-family permease and long sequences of SepJ; the corresponding tree including posterior probabilities for branch support is shown in Fig. S4, and taxa names are found in Table S5.

Figure 6. FRAP image sequence for a *Gloeocapsopsis* cell dyad loaded with Calcein-AM.

Top row: Bright-field image (grey-scale), chlorophyll fluorescence image (red) and merge of bright-field and chlorophyll fluorescence with calcein fluorescence (green). Scale-bar: 5 microns. Remaining panels show calcein fluorescence before bleaching (pre-bleach), after bleaching fluorescence in the left-hand cell (post-bleach) and then the same image with brightness enhanced for ease of visualisation. Images are then shown at the subsequent times indicated. Note that calcein fluorescence slowly equilibrates between the two cells.

699 The plot shows fluorescence in the bleached cell relative to the unbleached cell, versus
700 time. The line is an exponential curve fitted to the data points. See Fig. S6 for a second
701 representative example.
702
703

Journal of Bacteriology

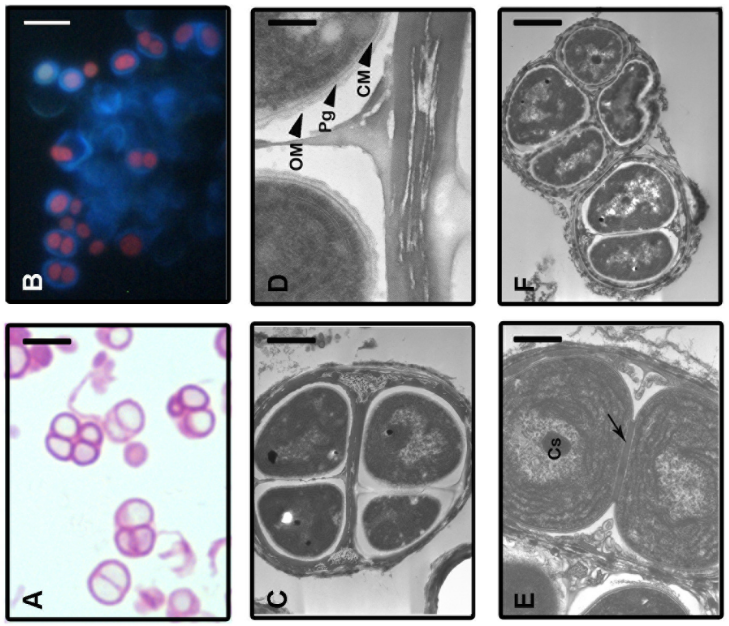

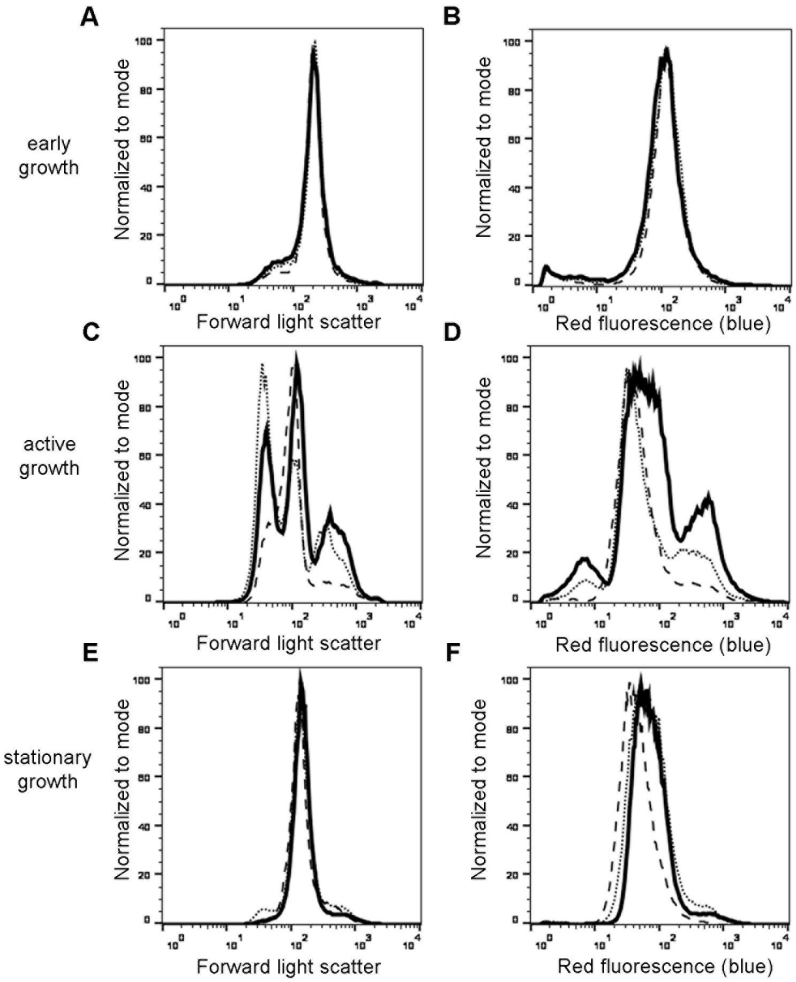

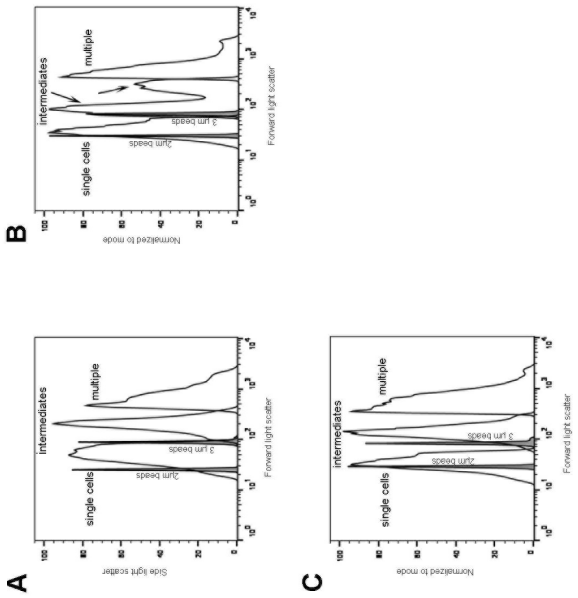

Journal of Bacteriology

JB

Journal of Bacteriology

				Multicellular septum formation							Other unknown gene exclusive of multicellular cyanobacteria (Stucken et al., 2010)						Heterocyst differentiation		
	Order	Family	Species	*sepJ* (*fraG*)	*fraE*	*fraC*	*fraD*	*fraH*	*amiC1*	*amiC2*	all2320 (CyDiv)	all1765	all1729	all2344	alr0202	alr4863	*hetR*	*patU3*	*hetZ*
Unicellular	Synechococcales	*Synechococcaceae*	*Synechococcus elongatus* PCC 6301	-	-	-	-	-	✓	-	-	-	-	-	-	-	-	-	-
			Synechococcus sp. CC9311	-	-	-	-	-	✓	-	-	-	-	-	-	-	-	-	-
		Prochlorococcaceae	*Prochlorococcus marinus* NATL2A	-	-	-	-	-	✓	-	-	-	-	-	-	-	-	-	-
			Prochlorococcus marinus pastoris CCMP 1986	-	-	-	-	-	✓	-	-	-	-	-	-	-	-	-	-
Filamentous, heterocystous	Nostocales	*Nostocaceae*	*Anabaena* sp. PCC 7120	✓	✓	✓	✓	✓	✓	✓	✓	✓✓	✓	✓	✓	✓	✓	✓	✓
			Nostoc azollae 0708	✓	✓	✓	✓	✓	✓	✓	✓	✓	✓	✓	✓	✓	✓	✓	✓
			Nostoc punctiforme PCC 73102	✓	✓	✓	✓	✓✓	✓	✓	✓	✓	✓	✓	✓	✓	✓	✓	✓
			Nostoc sp. PCC 7524	✓	✓	✓	✓	✓	✓	✓	✓	✓✓	✓	✓	✓	✓	✓	✓	✓
			Nostoc sp. PCC 7107	✓	✓	✓	✓	✓✓	✓	✓	✓	✓	✓	✓	✓	✓	✓	✓	✓
		Rivulariaceae	*Calothrix* sp. PCC7103	✓	✓	✓	✓	✓✓	✓	✓	✓	✓✓	✓	✓	✓	✓	✓	✓	✓
			Calothrix sp. PCC6303	✓	✓	✓	✓	✓✓	✓	✓	✓	✓✓	✓	✓	✓	✓	✓	✓	✓
			Fischerella sp. PCC9605	✓	✓	✓	✓	✓✓	✓	✓	✓	✓	✓	✓	✓	✓	✓	✓	✓
			Fischerella sp. PCC9339	✓	✓	✓	✓	✓✓	✓	✓	✓	✓	✓	✓	✓	✓	✓	✓	✓
Unicellular, tetrad-forming	Chroococcales	*Chroococcaceae*	*Gloeocapsopsis* sp. UTEX B3054	✓	✓	-	-	✓	✓	-	✓	✓✓	✓	-	-	-	-	-	-
			Gloeocapsa sp. PCC7428	✓	✓	-	-	✓	✓	-	✓	✓✓	✓	-	-	-	-	-	-
	Chroococcidiopsidales	Chroococcidiopsidaceae	*Chroococcidiopsis thermalis* PCC7203	✓	✓	-	-	✓	✓	-	✓	✓✓	✓	-	-	-	-	-	-